

Two body relaxation in CDM simulations

Juerg Diemand,^{*} Ben Moore, Joachim Stadel, Stelios Kazantzidis,

Institute for Theoretical Physics, University of Zürich ,CH-8057 Zürich, Switzerland

22 May 2019

ABSTRACT

N-body simulations of the hierarchical formation of cosmic structures suffer from the problem that the first objects to form always contain just a few particles. Although relaxation is not an issue for virialised objects containing millions of particles, collisional processes will always dominate within the first structures that collapse. First we quantify how the relaxation varies with resolution, softening, and radius within isolated equilibrium and non-equilibrium cuspy haloes. We then show how this numerical effect propagates through a merging hierarchy by measuring the local relaxation rates of each particle throughout the hierarchical formation of a dark matter halo. The central few percent of the final structures suffer from high degrees of relaxation - a region which one might naively think is well resolved at the final time since the haloes contains $\approx 10^6$ particles. The entire haloes have a degree of relaxation larger than unity which implies that the energy of any particle has been numerically changed by of order itself. We show that relaxation will flatten a cusp in just a few mean relaxation times of a halo. We explore the effect of resolution on the degree of relaxation and we find that increasing N slowly reduces the degree of relaxation $\propto N^{-0.25}$ rather than proportional to N as expected from the Vlasov equation. Cluster mass objects suffer most from relaxation since they form relatively late and therefore more of the particles spend more time in small N haloes.

Key words: methods: N-body simulations – methods: numerical – dark matter — galaxies: haloes

1 INTRODUCTION

A standard technique to study the formation and evolution of gravitating systems is to perform an N -body simulation in which the mass distribution is discretised into a series of softened point particles. This solution can be exact for a star cluster where each particle represents a single star, but for cosmological simulations of the dark matter each particle can be 10^{70} times larger than GeV mass candidates being simulated. In this approach the particles represent a coarse grained sampling of phase space which sets a mass and spatial resolution. Unfortunately these super-massive particles will undergo two body encounters that lead to energy transfer as the system tends towards equipartition. In the real Universe the dark matter particles are essentially collisionless and pass unperturbed past each other.

The processes of relaxation is difficult to quantify, but in the large N limit the discreteness effects inherent to the N-body technique vanish, so one tries to use as large a number of particles as computationally possible. Increasing the mass resolution of a given simulation allows a convergence test of properties such as the dark matter density profile

i.e. Moore et al. (1998), Ghigna et al. (2000), Klypin et al. (2001) and Power et al. (2003). These authors find that to resolve the central 1 per cent of a dark matter halo the entire system must contain of the order a million particles. It is not known what process sets this resolution scale since with one million particles relaxation is expected to be small, even at 1 per cent of the virial radius.

Unfortunately in most cosmological simulations the importance of two body interactions does not vanish if one increases N . Structure formation in the cold dark matter (CDM) model occurs hierarchically since there is power on all scales, so the first objects that form in a simulation always contain only a few particles (Moore et al. 2001), (Binney & Knebe 2002). With higher resolution the first structures form earlier and have higher physical densities because they condense out of a denser environment. Two body relaxation increases with density, so it is not clear if increasing the resolution can diminish the overall amount of two body relaxation in a CDM simulation, i.e. if testing for convergence by increasing the mass resolution is appropriate.

In isolated equilibrium systems relaxation rates can be measured from the energy dispersion. In cosmological simulations one can measure the amount of mass segregation

^{*} diemand@physik.unizh.ch

of multi-mass simulations (Binney & Knebe 2002) where lighter particles gain more energy from collisional processes than the heavier particles. In Section 2 we present a Fokker-Planck type relaxation time estimate, which was fitted to a series of test simulations (Section 3.1) where we explore the relaxation rates as a function of N , radius and softening parameter in both equilibrium and non-equilibrium cuspy haloes. We then use this local relaxation rate estimate to follow the relaxation history of each particle during 1000 time-steps of a hierarchical CDM simulation. The resulting degree of relaxation as a function of spatial position within galaxy and cluster mass haloes is analysed in Section 4 and in Section 5 we discuss the effects that relaxation has on haloes at $z = 0$.

2 A LOCAL RELAXATION TIME ESTIMATE

In this paper we adopt the energy definition of the relaxation time (Chandrasekhar 1942) stating that the mean relaxation time T of a group of stars is the time after which the mean square energy change due to successive encounters equals the mean kinetic energy of the group. Note that this time is half of the relaxation time T_v defined in Binney & Tremaine (1987) who calculate a mean velocity change, because $\Delta E^2/E^2 \simeq 2\Delta v^2/v^2$. The orbit averaged Fokker-Planck estimate for T_v is

$$T_v = 0.34 \frac{\sigma^3}{G^2 m \rho \ln \Lambda}, \quad \Lambda \equiv \frac{b_{max}}{b_{min}}, \quad (1)$$

where σ is the one dimensional velocity dispersion, ρ the density and m the particle mass. The parameters b_{min} and b_{max} are the minimum and maximum limits for the impact parameter.

We use a similar formula evaluated for each particle using its 16 nearest neighbours as a local estimate for the relaxation time T_{LE} , and the local relaxation rate r_{LE} :

$$T_{LE} = \frac{1}{r_{LE}} = \gamma \frac{\sigma^3}{G^2 m \rho C}, \quad \gamma \equiv 0.17. \quad (2)$$

The value of γ , and the parameters in the Coulomb logarithm C are chosen to roughly fit measured relaxation times of equilibrium haloes, see section (3).

$$C \equiv 0.5 \left[\ln(1 + \Lambda^2) - \frac{\Lambda^2}{1 + \Lambda^2} \right] (\simeq \ln \Lambda, \text{ if } \Lambda \gg 1), \quad (3)$$

the analytical calculation for Newtonian potentials shows that $b_{min} = b_0 = 2Gm/v_{rel}^2$, b_0 is the impact parameter where the deflection angle reaches $\pi/2$ (Bertin 2000). In a softened potential the scattering calculation has to be done numerically and the results agree roughly with the Newtonian case if one sets $b_{min} = \epsilon$, i.e. one ignores all encounters with an impact parameter smaller than the softening length (Theis 1998). We set

$$b_{min} \equiv \max(Gm/3\sigma^2, \epsilon) \simeq \max(b_0, \epsilon), \quad (4)$$

because $\overline{v_{rel}^2} = 6\sigma^2$. The proper choice of b_{max} is controversial, it is not clear whether it should be related to the size of the whole system or to the mean interparticle distance. For cosmological simulations we prefer the second choice

$$b_{max} \equiv \beta(m/\rho)^{1/3} \quad (5)$$

because this is a local quantity that is easy to measure and less ambiguous than defining the size of irregular shaped, collapsing structures.

We calculate the local velocity dispersion and density surrounding each particle by averaging over its 16 nearest neighbours. We do a simple top-hat average, because using an SPH spline kernel leads to biased results when using only 16 particles. We found good agreement with all measurements when using $\beta = 10$ and $\gamma = 0.17$. Averaging over different numbers of nearest neighbours the optimal parameters differ slightly due to different amounts of numerical noise in the local density and velocity dispersion.

3 TWO BODY RELAXATION IN SPHERICAL HALO MODELS

In this section we present a number of test cases and show that the local relaxation estimate agrees quite well (within 15 per cent) with measured relaxation times for a wide range of particle numbers, softening lengths and virial ratios. This range covers the haloes that form in cosmological simulations, however all the test cases are isotropic, spherical haloes. Haloes in cosmological simulations are close to isotropic, but are triaxial and contain substructures. But one can argue that locally the two are similar, and if a local relaxation time estimate works in the spherical haloes, it should give a reasonable estimate also in the cosmological case.

3.1 Equilibrium haloes

In an equilibrium model the energy of each particle would be conserved in the $N \rightarrow \infty$ limit. For finite N the energies of particles suffer abrupt changes due to encounters. Therefore we can directly measure the relaxation time with

$$T = \Delta t \frac{\overline{E_{kin}}^2}{\Delta E^2(\Delta t)}, \quad (6)$$

where $\Delta E(\Delta t)$ is the energy difference of one particle after time interval Δt and the bar denotes the group average.

Here we present a sequence of tests using spherical and isotropic Hernquist models (Hernquist 1990) which are a reasonable approximation to the haloes found in cosmological N-body simulations. (We found no difference between these simulations and tests using NFW and Moore profiles, constructed by solving for the exact phase space distribution function numerically as described in Kazantzidis, Magorrian & Moore (2003).) The density profile of the Hernquist model is

$$\rho(r) = \frac{M}{2\pi} \frac{a}{r} \frac{1}{(r+a)^3}. \quad (7)$$

We set ¹ the total mass to $M = 3.5 \times 10^9 M_\odot$ and the scale length to $a = 10$ kpc. Then the half mass radius is $r_h \simeq$

¹ To rescale the results to different size haloes just change the distance scale by some factor $x \rightarrow fx$, mass scale $M \rightarrow f^3 M$ and the dynamical and relaxation timescales do not change. To rescale to different timescales $T \rightarrow cT$ do $M \rightarrow c^{-2} M$ with fixed length scale.

$2.4a = 24$ kpc and the crossing time at half mass radius is $T_c \equiv r_h/v_{circ}(r_h) \simeq 1.3$ Gyr.

All the simulations have been carried out using PKDGRAV, a state of the art, multi-stepping, parallel tree-code (Stadel 2001). The time-steps are chosen proportional to the square root of the softening length over the acceleration on each particle, $\Delta t_i = \eta \sqrt{\epsilon/a_i}$. We use $\eta = 0.25$, and a node-opening angle $\theta = 0.55$ for all runs in this section, except the long term integrations in subsection 3.3 where we use $\eta = 0.03$. Energy conservation was better than 0.1 per cent after several crossing times for all runs in this section.

Due to softening the initial models are not exactly in equilibrium, the total kinetic energy is a few percent larger than half of the potential energy. For this reason we evolved the models for five crossing times before measuring the energy dispersion, which results in up to 10 per cent longer relaxation times.

Figure 1 shows $\overline{\Delta E^2(\Delta t)}$ as a function of time within haloes constructed with $N = 10^4$ and $N = 100$ particles. The upper panel shows that for small numbers of particles $N \ll 10^3$ $\Delta E(\Delta t)$ becomes very noisy since there are fewer, but more significant encounters. To obtain more reliable results in small N groups we added a sufficiently large number (10^4) of massless tracer particles following the same distribution in real and velocity space as the massive particles. The open squares in Figure 1 show the 'energy' dispersion of the tracers, which in large N groups is just the same as the energy dispersion of the massive particles, but it evolves much smoother with time in small N groups. We obtain the mean relaxation times (6) of these haloes with linear fits to the energy dispersion of the tracer particles (open squares), taking into account points where $\Delta E^2 < 0.2$, i.e. in the upper panel only the points right of the vertical bar, to make sure that Δt is small compared to the relaxation time.

Note that the tracers are not in equilibrium with the halo, on average they gain speed in encounters and are ejected from the core. Typically after one relaxation time the number of tracers inside of $r = a$ drops to one half of the initial number. Therefore it is important to use a Δt shorter than T and to add the tracers after evolving the halo for five crossing times, otherwise the relaxation in the core is not sufficiently reflected in the energy dispersion of the tracers and T could be underestimated significantly.

3.1.1 Dependence on N and ϵ

Figures 2 and 3 show the measured mean relaxation times as a function of N and softening parameter, ϵ , compared with the local estimate (2). We find that the measured relaxation times are proportional to N (dashed reference line), rather than to $N/\ln(N)$ (dotted line), as expected for a softened potential. The same result was found for King models by Huang, Dubinski & Carlberg (1993). The local estimate of the relaxation time increases slightly faster with N than the measured values. This is due to the fact that we choose a maximum impact parameter proportional to the mean interparticle separation, i.e. $b_{max} \propto N^{-1/3}$, but the difference is less than 10 per cent for all relaxation times shorter than a Hubble time, i.e. for $N \leq 10^4$.

The dependence on the softening length is shown in Figure 3 for a $N = 10^4$ model. The measured values (filled squares) increase faster with ϵ than the local estimate (open

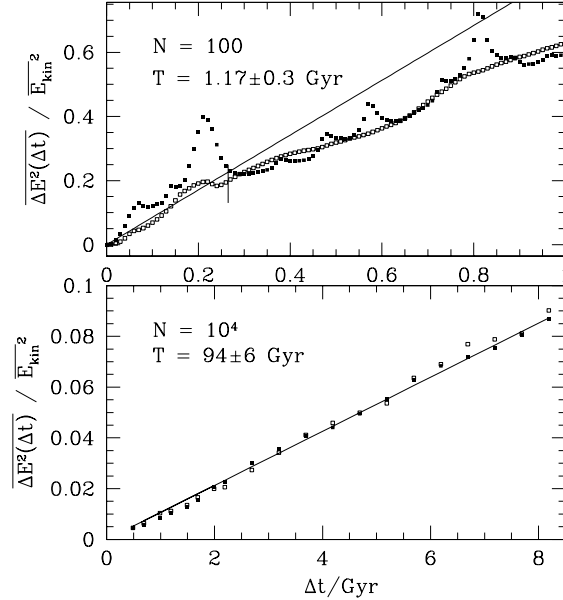


Figure 1. Mean squared energy change $\overline{\Delta E^2(\Delta t)}$ as a function of time. The filled squares show the mean squared energy change of the actual particles, the open squares for the massless tracer particles. The lines are linear fits to the mean squared energy change of the tracers, in the upper panel only the points right of the vertical bar are taken into account.

squares) (like in Figure 2 of Huang et al. 1993), but the differences are small ($\gtrsim 15$ per cent) for realistic softenings $\epsilon \lesssim 0.1a = 1$ kpc. The average relaxation time of this model increases from 30 Gyr to 180 Gyr when the softening parameter is changed from 0.01 kpc to 1 kpc. This is slightly higher than expected from the scaling with $\ln(\epsilon)$ since the density profile and central cusp are better resolved with smaller softening.

3.1.2 Dependence on radius

Measuring the relaxation time as a function of radius $T(r)$ proved to be quite difficult. The most credible method seems to take (6) and replace the average over all particles by the average over those, which are in the corresponding radial bin at the beginning (or at the end) of the time interval Δt . Clearly one has to choose $\Delta t \ll \delta r/\sigma(r)$, where δr is the size of the bins, to make sure that most particles spend most of Δt in the same bin. This could also be reached also by placing the tracers on circular orbits, which leads to very similar results for $T(r)$ if $r \sim r_h$, but in the centre this method fails, because there the circular velocity is much smaller than the velocity dispersion².

In Figure (4) we plot the relaxation rate against radius

² From a convolution of the velocity distributions one finds that the relative velocities in encounters with tracers on circular orbits have a different dispersion ($\sigma_{v_{rel}}^2 = 3\sigma^2 + v_{circ}^2$) than those of encounters between the massive particles ($\sigma_{v_{rel}}^2 = 6\sigma^2$). In non isothermal haloes, $3\sigma^2 \neq v_{circ}^2$ and this leads to systematic errors in the measured relaxation times. In Hernquist models $3\sigma^2 \sim v_{circ}^2$ holds only for $r \sim r_h$, and indeed we found good agreement with the other methods only in this range.

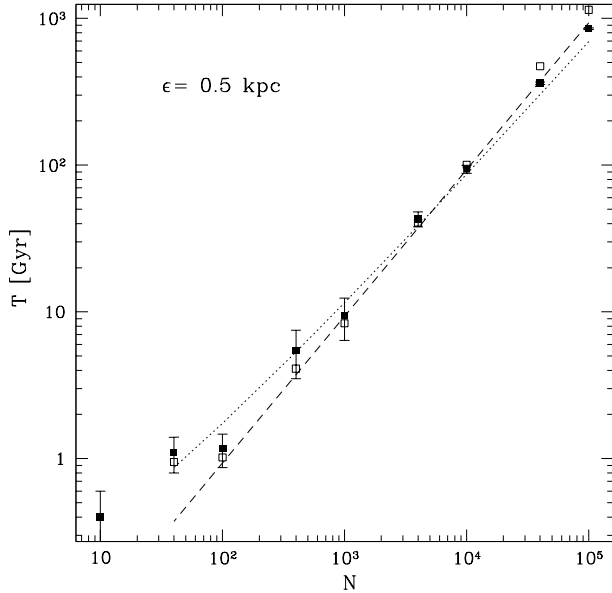


Figure 2. Average relaxation times of isotropic Hernquist models versus particle number N , with a constant softening $\epsilon = 0.5$ kpc. The filled squares are the measured relaxation times, with error bars from the linear fit of $\overline{\Delta E^2}(\Delta t)$. The open squares are the local estimates of the relaxation time (2).

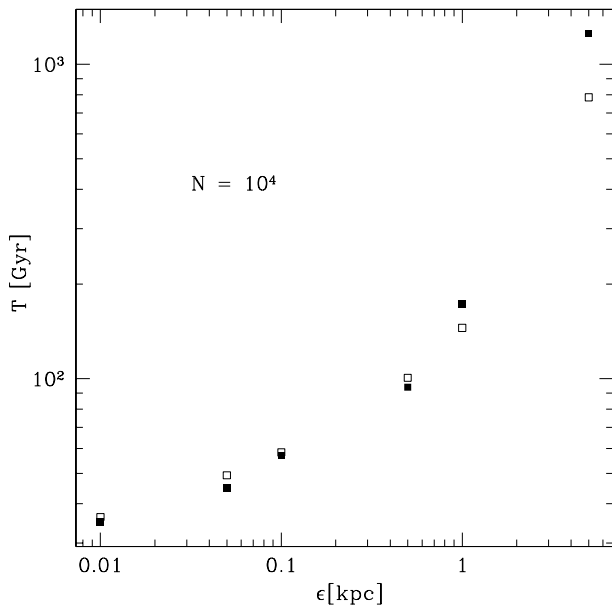


Figure 3. Average relaxation times of an $N = 10^4$ Hernquist models versus softening length ϵ . The filled squares are the measured relaxation times, the open squares are the local estimate (2).

for a Hernquist model with 10^4 particles. We measured the energy dispersion (filled squares) during $\Delta t = 0.1$ Gyr for each particle, and averaged the values of particles starting in the same radial bin. We also measured the local relaxation rate r_{LE} (2) at 100 time-steps during Δt for each particle and summed them up. The radial averages are plotted with open squares. Again the agreement with the measured en-

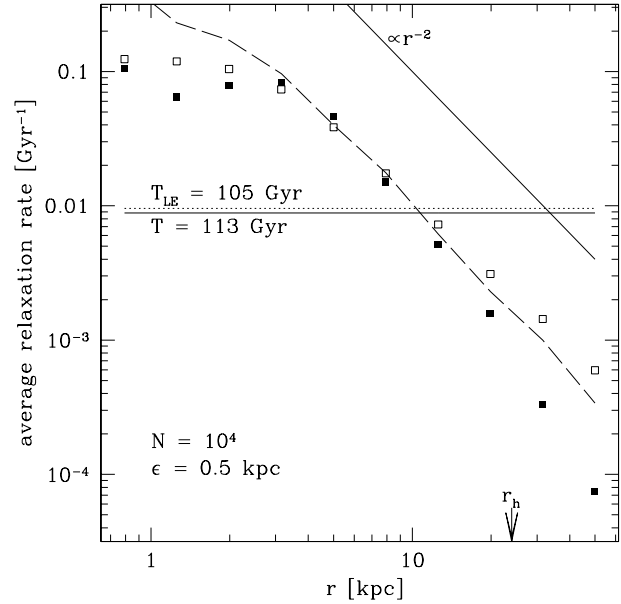


Figure 4. Relaxation rate of an $N = 10^4$ halo vs. radius. The filled squares are the measured relaxation, the open squares are the local estimate r_{LE} , calculated from 16 nearest neighbours during 0.1 Gyr. The horizontal lines give the halo averages of measured (solid line) and estimated (dotted line) relaxation rates. We also plot $2/T_v$ (dashed line) calculated from all particles in the radial bin.

ergy changes is better than 35 per cent except in the last three bins where the relaxation rates are many thousands of Gyrs and the local relaxation measurement overestimates the true rate of relaxation. In the inner three bins the crossing times are shorter than 0.2 Gyr, i.e. many of the particles had time to move through these bins during $\Delta t = 0.1$ Gyr.

The dashed line is the inverse of half the Fokker-Planck estimate (1) with $\Lambda = r_h/\epsilon$, calculated using all particles in the bin, not only from 16 nearest neighbours. It scales like the phase space density $\rho(r)/\sigma^3(r) \propto r^{-2}$, the same holds for the local estimate in the seven outer bins. The measured relaxation scales more like $\propto r^{-3}$ in the outer region, but the slope depends strongly on Δt , i.e. on how many particles from the core with 100 times higher relaxation rate have had time to reach the outer region.

The average relaxation times³ are about 10 times shorter than measured relaxation times at half mass radius, due to the fast relaxation in the high density core of cuspy haloes. For a less concentrated King model ($\Psi_0 = 5$) the Fokker-Planck estimate seems to agree not only with the measured relaxation time at half mass radius, but also with the mean relaxation time (Huang et al. 1993).

³ Note that analytically the average of the relaxation rate estimate r_{LE} (1) is divergent for models with central cusps $\propto r^{-1}$ and steeper: $T = \int_0^R r_{LE}(r)\rho(r)r^2dr \propto \int_0^R r^{-2}\rho(r)r^2dr = \int_0^R \rho(r)dr$.

3.2 Collapsing haloes

Instead of setting up initial conditions of the tracers exactly like those of the massive particles, one can also restrict the tracers to a common orbital plane. This does not change their density profile nor the relative velocities in encounters with the massive particles. If we choose the orbital plane of the tracers to be the xy -plane, then the energy dispersion is

$$\frac{\overline{\Delta E^2}}{E_{kin}^2} \simeq \frac{\overline{\Delta E_{kin}^2}}{E_{kin}^2} \simeq 2 \frac{\overline{v_z^2}}{\overline{v^2}} = 4 \frac{\overline{v_z^2}}{\overline{v^2}}, \quad (8)$$

as long as $\overline{v_z^2} \ll \overline{v^2}$, i.e. for small time intervals. This relates the energy dispersion to a more demonstrative quantity and in the edge on view of the xy -plane one can actually observe the relaxation process since the degree of relaxation is roughly proportional to the thickness of the disk.

With (8) we can also attempt to measure relaxation times in non-equilibrium situations, we only need spherical symmetry to be able to apply this method. In CDM simulations the virial ratio $\alpha \equiv 2E_{kin}/|E_{pot}|$ is close to zero at the beginning of a halo collapse and grows towards unity as the halo reaches dynamical equilibrium. In the previous sections we showed that the local estimate (2) works for $\alpha = 1$, but for $\alpha \rightarrow 0$ the phase-space density $\propto \alpha^{-1.5}$ goes to infinity. Down to which virial ratio can we trust our local estimate?

To answer this question we began with equilibrium Hernquist models (same parameters as in section 3.1.1) with 10^4 particles and multiplied all velocities with $\sqrt{\alpha}$. To these models we added 10^4 massless tracer particles with the same phase-space distribution and tilted their orbital planes into the xy -plane. Then we measure $\overline{v_z^2}/\overline{v^2}$ and the local estimate (2) at 100 time-steps during the first 0.1 Gyr of the collapse. Linear fits give the relaxation times plotted in Figure (5), the dashed line shows the scaling $\propto \alpha^{1.5}$ expected from the Fokker-Planck type estimates (1) and (2). Our relaxation time estimate becomes very small when the virial ratio goes to zero, but the measured relaxation times remain on the order of a few dynamical times. T_{LE} is within a factor of two for $\alpha \gtrsim 0.075$ and within 10 per cent for $\alpha \gtrsim 0.5$.

3.3 Evolution of isolated Halos

The dynamical evolution of globular clusters is driven by relaxation, which can lead to core collapse and evaporation on a timescale of a few tens of half mass relaxation times, i.e. the core loses energy to an expanding outer envelope of stars and gets denser and hotter (Binney & Tremaine 1987, Spitzer 1987).

In the next section we show that haloes in cosmological simulations are typically between one and ten mean relaxation times old. (In terms of the much longer half mass relaxation time they are younger than one or two half mass relaxation times.) Therefore we do not expect that density profiles in cosmological simulations are significantly affected by the core collapse process.

Studies of globular cluster evolution start with models that are isothermal in the centre (e.g. Plummer spheres, King models) and then show a slow but monotonic density increase in the core. In contrast the cuspy haloes in cosmological simulations are not isothermal: the velocity dispersion decreases in the central regions. In this case relaxation leads to an energy flow inwards, the core evolves towards a

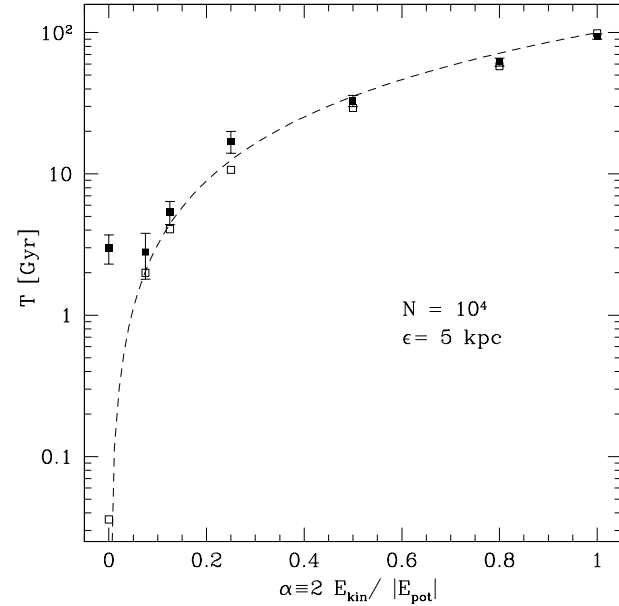


Figure 5. Relaxation times of a $N = 10^4$ non-equilibrium Hernquist model vs. virial ratio. The filled squares are measured with $\overline{v_z^2}/\overline{v^2}$, the open squares are the local estimate (2). The reference line is $\propto \alpha^{1.5}$.

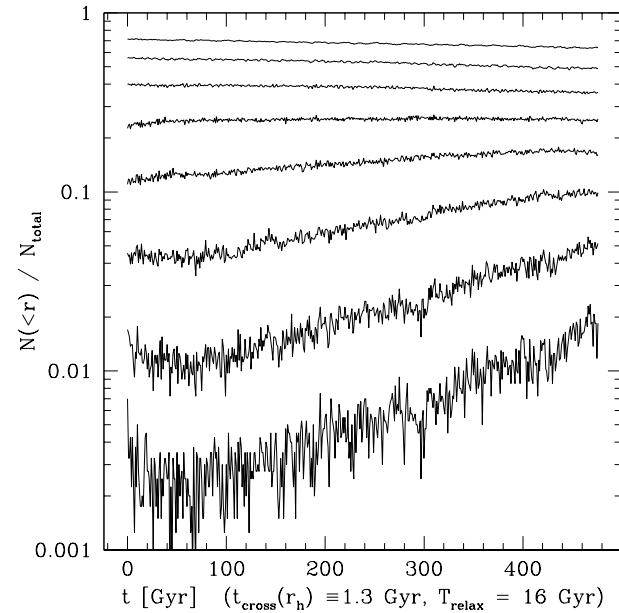


Figure 6. From top to bottom, the mass fraction within 0.89, 1.58, 2.81, 5.00, 8.90, 15.8, 28.1 and 50.0 kpc of five $N = 4'000$ Hernquist models vs. time.

less dense, isothermal state first. Later the system evolves just like the models in globular cluster calculations. The N-body simulations of Hayashi et al. (2003) show this evolution starting from an NFW profile. We confirmed their result by evolving an $N = 4'000$ Hernquist model for 360 crossing times (see Figure 6).

Figure 7 shows the evolution of five $N = 4'000$ Hernquist models during 50 Gyr, using a softening of $\epsilon = 0.1$ kpc. For this long term evolution we use a more conservative time

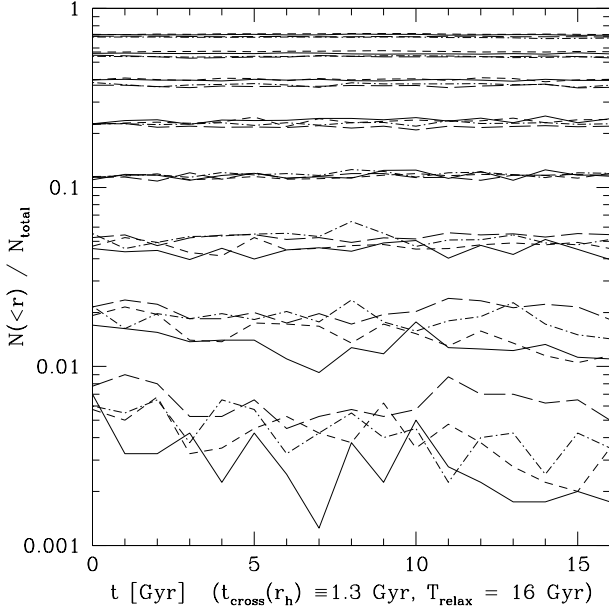


Figure 7. From top to bottom, the mass fraction within 0.89, 1.58, 2.81, 5.00, 8.90, 15.8, 28.1 and 50.0 kpc of five $N = 4'000$ Hernquist models vs. time.

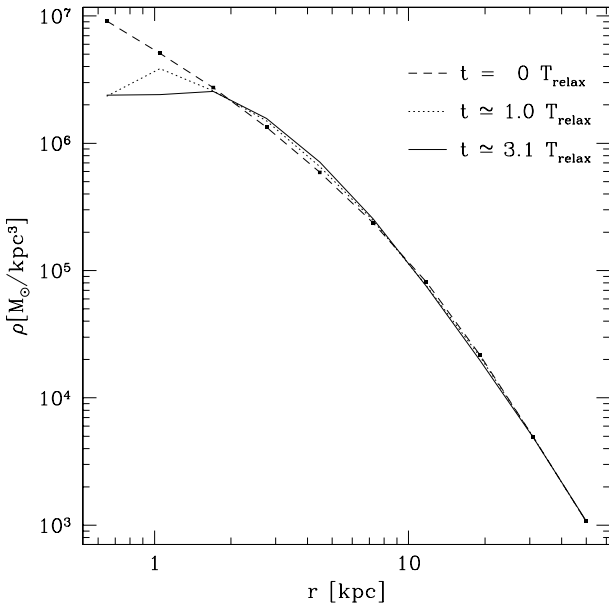


Figure 8. Averaged density profiles of five $N = 4'000$ Hernquist models (same models as in Figure 7), initial profile (dashed line), after 16 Gyr (dotted line) and after 50 Gyr (solid line). The points indicate the radius of the outer borders of the spherical bins.

step parameter $\eta = 0.03$, energy is conserved within 0.36 per cent even after 360 crossing times. The crossing time at the half mass radius is 1.3 Gyr, the initial mean relaxation time is 16 Gyr and the initial half mass relaxation time is 71 Gyr. After 50 Gyr this halo is about three mean relaxation times old, a realistic value for haloes in current cosmological simulations, see section (4). The same would happen to a $N = 100$ halo in only 1.25 Gyr, we use $N = 4'000$ just to have a well defined density profile down to $0.1a = 1$ kpc.

During this 50 Gyr, the velocity dispersion in the centre rises and at the scale radius it drops slightly, in the end the core is already close to isothermal. This energy gain is compensated with core expansion, the inner two mass shells plotted in Figure 7 clearly lose mass. This is not a numerical artifact, the softening we used is much smaller than the inner bin and in a $N = 4 \times 10^4$ reference model the mass loss in the inner two bins is about ten times slower, i.e. this is really an effect driven by relaxation. The corresponding density profiles are less steep in the inner 3 per cent of the halo, see Figure 8, and show constant density cores in this region.

4 RELAXATION IN COSMOLOGICAL SIMULATIONS

Here we present results from four small to medium resolution Λ CDM simulations ($\Omega_\Lambda = 0.7$, $\Omega_m = 0.3$, $\sigma_8 = 1.0$). We generate initial conditions with the GRAFIC2 package (Bertschinger 2001). We start with a 128^3 particle cubic grid with a comoving cube size of 60Mpc (particle mass $m_p = 3.6 \times 10^9 M_\odot$). Later we refined two interesting regions, in the first one a cluster halo ($M_{200} = 7.4 \times 10^{13} M_\odot$, $r_{200} = 1440$ kpc) forms, the refinement factors are 2 and 3 in length, i.e. 8 and 27 in mass (run C2,C3). In the second region a galaxy size halo ($M_{200} = 1.4 \times 10^{12} M_\odot$, $r_{200} = 350$ kpc) forms. There we used a refinement of 9 in length, i.e. 729 in mass, and included a buffer region, about 2 Mpc deep, with an intermediate refinement factor of 3 (run G9). We start the simulations when the standard deviation of the density fluctuations in the refined region reaches 0.2. The softenings used in the refined regions are $\epsilon = 1.86$ kpc for the cluster and $\epsilon = 0.5$ kpc for the galaxy, i.e. $\epsilon \simeq 0.0013 r_{vir}$ in both cases. We also run the unrefined cube again with this softening in the cluster forming region (run C0). The numerical parameters are as in section 3.1, but at late epochs we use a larger node-opening angle to speedup the runs, $\theta = 0.7$ for $z < 2$.

In non equilibrium, non spherical haloes of a cosmological simulation it is not possible to measure two body relaxation times with the methods used in section 3. Binney & Knebe (2002) used initial conditions with two species of particles with different mass. Both species start from a regular lattice, such that the nodes of one grid are at the centres of the cells of the other, and both are then displaced according to the Zel'dovich approximation. In a collisionless simulation the final distribution of the particles would be independent of mass. They found differences in the number density of the light and heavy particles in the centres of haloes. However it is not clear that a mass segregation in a poorly resolved early progenitor survives the mergers and contributes to the number density difference observed at $z = 0$. Imagine a small N progenitor with a core that is many relaxation times old and has developed an evident mass segregation. According to section 3.3 its core has expanded and is less dense. Therefore tidal stripping disrupts this progenitor before it reaches the centre, and the central mass segregation of the remnant is unchanged.

We assign a degree of relaxation to each particle, which is calculated after each of 1000 fixed time-steps Δt from the local relaxation rate estimate (2) and summed up over the whole cosmological simulation

Table 1. Average Degrees of Relaxation

Run	C0	C2	C3	G9
N_{200}	20'500	177'000	650'000	250'000
d_0 inside $0.1r_{200}$	5.98	3.62	3.06	1.67
d_0 inside r_{200}	5.23	3.34	2.52	1.15
d_{TA} inside $0.1r_{200}$	4.74	2.40	1.78	0.72
d_{TA} inside r_{200}	3.67	2.42	2.12	1.02
d_{VIR} inside $0.1r_{200}$	3.58	1.61	1.17	0.42
d_{VIR} inside r_{200}	2.50	1.52	1.34	0.58

$$d_0 := \sum_{n=1}^{1'000} r_{LE}(t_n) \Delta t. \quad (9)$$

As shown in section 3.2, r_{LE} reflects the measured relaxation rates only for virial ratios $\alpha \gtrsim 0.1$. Since this is not case for the first steps in a CDM simulation, we set r_{LE} to zero before the local density reaches some threshold. When the local density reaches $6\rho_0$ (\simeq density at turnaround in the spherical collapse) the typical values for α are close to 0.4, later at $170\rho_0$ (\simeq density at virialisation in the spherical collapse) α is close to unity. We used these two density thresholds, in the first case we write d_{TA} for the ‘‘degree of relaxation since turnaround’’, otherwise d_{VIR} for ‘‘degree of relaxation since virialisation’’. The relaxation averages over all particles inside r_{200} and $0.1r_{200}$ at $z = 0$ are given in table 1.

4.1 Number of particles

A reassuring result is that with more particles the simulations are less affected by two-body relaxation, even though one resolves more small N progenitors. This confirms the significance of convergence tests that vary the number of particles. The average degree of relaxation inside of $0.1r_{200}$ scales like $N^{-0.3}$, and the relaxation inside of r_{200} like $N^{-0.2}$.

Figure 10 shows the relaxation in the cluster as a function of the final particles position, for three different resolutions. In the outer part ($r \gtrsim 0.1r_{200}$) the cluster has substructure, which are small N systems that exist at the present time, so they are still relaxing at a high rate at $z = 0$ (bottom panel). Substructure haloes with $N \simeq 500$ can reach averages of $d_{\text{VIR}} \simeq 10$ in all runs, the highest peaks in d_{VIR} are found in the centre of substructure haloes, where d_{VIR} can be as high as 100, much higher than in the centre of the host halo (see Figure 9).

Note that the degrees of relaxation (top and middle panel) are much larger than what you would estimate using the final distribution of particles (bottom panel). Other studies consider only the relaxation rate at $z = 0$, and claim to resolve a halo down to a radius where this relaxation time $r_{LE}^{-1}(z = 0)$ is larger than Hubble time (Power et al. 2003) or larger than three Hubble times (Fukushige & Makino 2001). This radius scales $\propto N^{-0.5}$, whereas convergence in N-body simulations seem to be slower; In Moore et al. (1998) and Ghigna et al. (2000) the resolved radii are determined by comparing density profiles between simulations with different numbers of particles. They found that the ‘‘resolved radius’’ $r \simeq 0.5N_{200}^{-0.3}$ for a wide range of N_{200} fromm 10^2 to $10^{5.7}$. It appears like the resolved radius scales in the same

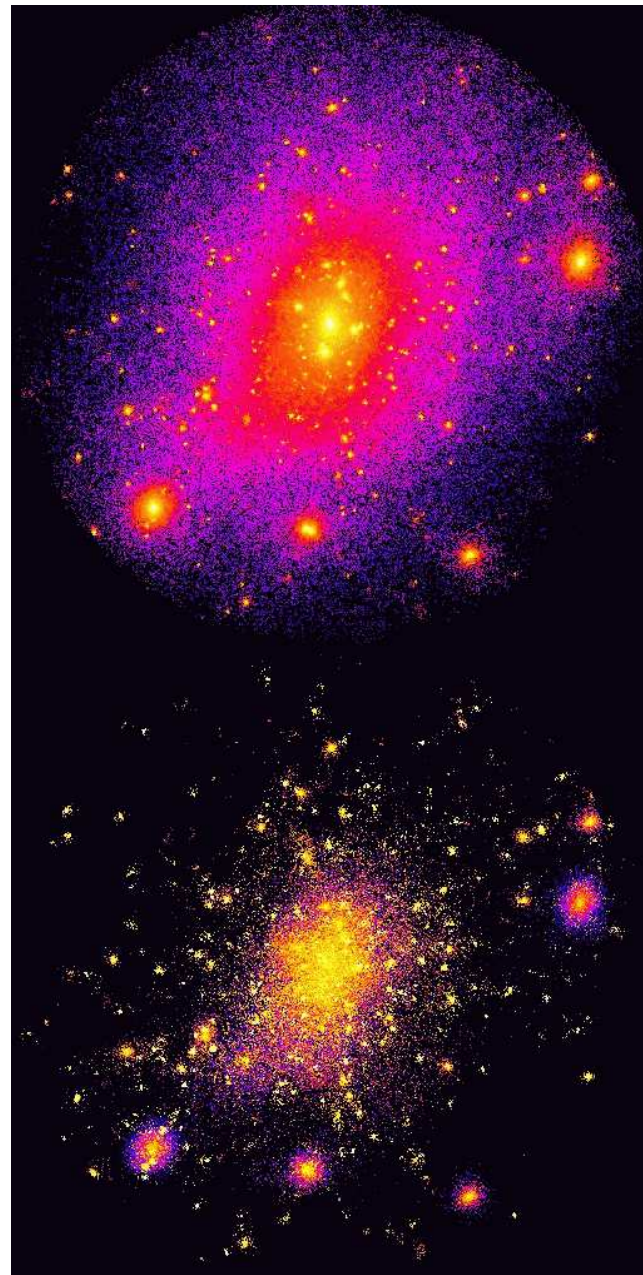


Figure 9. Maps of the cluster’s density (top) and relaxation since virialisation (bottom) out to r_{200} for the C3 run ($N_{200} \simeq 650'000$). The logarithmic scale for the degree of relaxation goes from 0.01 (black) to 100 (white).

way as the average degree of relaxation, but further relaxation studies for a wider range N are needed to verify this.

4.2 Mass and time dependence

Figure 11 compares the relaxation rate within the high resolution cluster and the galaxy simulations. The average degree of relaxation at $z = 0$ for the galaxy ($d_{\text{VIR}} \simeq 0.58$) is much smaller than for the cluster ($d_{\text{VIR}} \simeq 1.34$), even though N is larger for the cluster and therefore the present relaxation rate $r_{LE}(z = 0)$ is smaller in the cluster. The reason is that the cluster forms much later than the galaxy

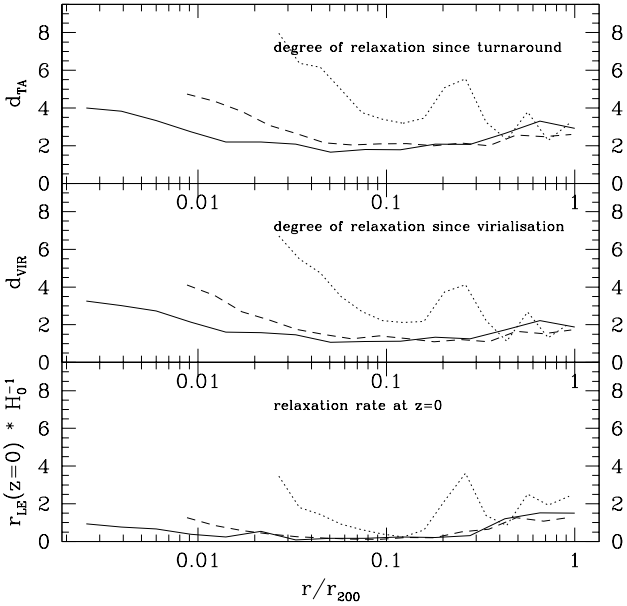


Figure 10. Relaxation versus radius. The solid line is for run C3, the dashed line for run C2 and the dotted line for run C0.

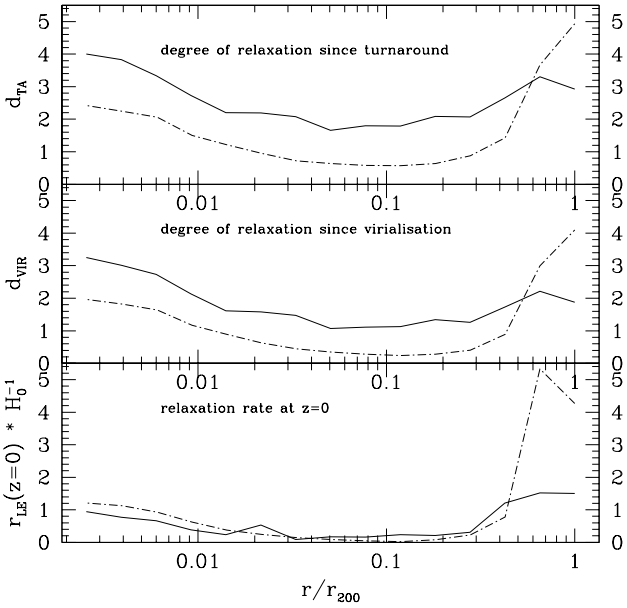


Figure 11. Relaxation vs. radius. The solid line is the cluster run C3 ($N_{vir} \simeq 650'000$), the dot - dashed line for the galaxy ($N_{vir} \simeq 250'000$).

therefore most of its particles have spent a longer period of time in small N progenitor haloes.

In Figures 12 and 13 we plot how the degree of relaxation increases with time for both haloes for particles within 10 per cent of the virial radius and for all the particles within the virial radius. Most of the relaxation within the central region of the galaxy occurs within the first couple of Gyrs of the evolution of the Universe. The cluster forms over a longer timescale and this is reflected in the longer increase in the degree of relaxation with time.

The cluster runs (C0,C2,C3) show how relaxation in

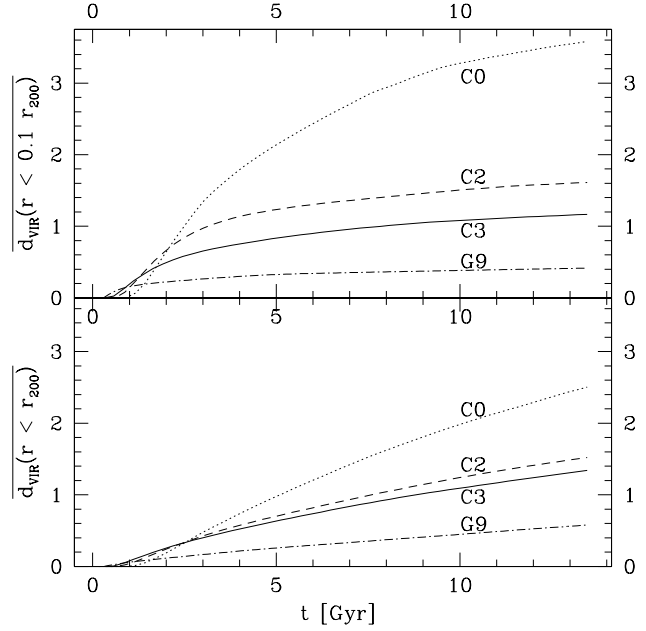


Figure 12. The degree of relaxation, d_{VIR} , averaged over all particles as a function of time. In the top panel we average over particles inside $0.1 r_{200}$ at $z = 0$ and in the bottom panel over all inside r_{200} .

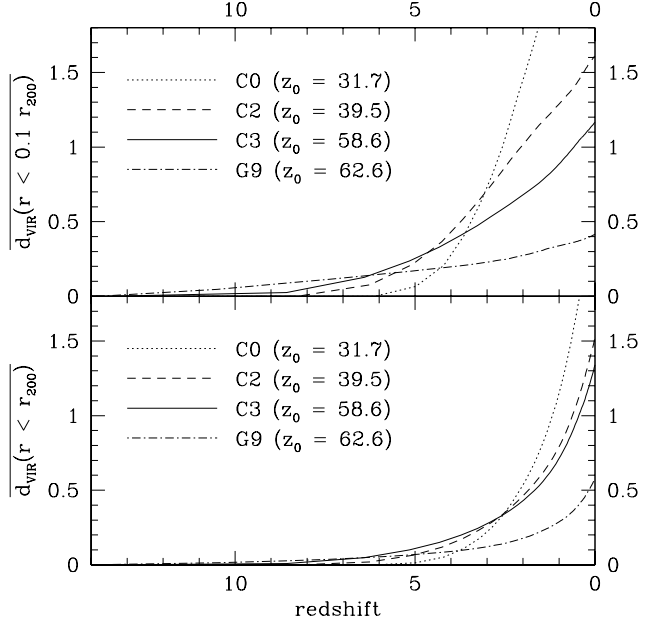


Figure 13. Same as Figure 12 but as a function of redshift. z_0 is the starting redshift of the runs.

small N groups starts earlier, after 1 Gyr the highest resolution run (C3) is most affected by relaxation. This result is not an artifact from using a density threshold, we checked that the d_0 shows the same behaviour as d_{VIR} . The entire haloes (bottom panel) show some relaxation during the whole simulation which arises from the poorly resolved substructure haloes in the outer regions.

5 DISCUSSION & CONCLUSIONS

N-body cosmological simulations attempt to model a collisionless system of particles using a technique that is inherently collisional on small scales. We have examined the relaxation rates of isolated equilibrium cuspy haloes as a function of particle number, radius and softening parameter. We show how one can define a local relaxation timescale for each particle by measuring its local phase space density which allowed us to follow the relaxation histories of all the particles in a hierarchical cosmological simulation of galaxy and cluster mass haloes. We summarise our results here:

- (i) The mean relaxation rates in cuspy dark matter haloes increases linearly with time at the same rate predicted by the orbit averaged Fokker-Planck equation. However the average relaxation time is an order of magnitude less than that measured at the half mass radius.
- (ii) The relaxation time is proportional to the local phase space density which allows us to measure the cumulative amount of relaxation each particle undergoes during the evolution of a halo.
- (iii) We verify that the average relaxation time of a halo is proportional to the number of particles it contains.
- (iv) We show that we can measure the relaxation rate in collapsing or non-equilibrium haloes that have kinetic to potential energy ratios up to ten times the equilibrium value.
- (v) Averaging over several simulations of cuspy Hernquist haloes we show that within few mean relaxation times the central cusp is transformed into a constant density core.
- (vi) We show that the hierarchical build up of galaxy or cluster mass haloes leads to a greatly enhanced degree of relaxation at all radii which is of the order of unity.
- (vii) Cluster haloes suffer three times the amount of relaxation as galaxy haloes simulated at the same spatial and mass resolution. This is because the cluster forms later and more of its particles spend time in poorly resolved progenitors.
- (viii) Increasing the resolution (N) at a fixed force softening reduces the the accumulated amount of relaxation – the average degree of relaxation in CDM haloes at $z = 0$ scales $\propto N^{-0.2}$, in the inner 10 percent $\propto N^{-0.3}$. Relaxation can therefore provide a simple explanation for the convergence in density profiles of CDM haloes simulated at different resolutions. This also explains why convergence studies demonstrate that we need 10^6 particles to resolve down to one percent of a CDM halo.
- (ix) Most of the affected particles become “relaxed” very early and within the first few Gyrs of the evolution of the Universe. This is hardest epoch to accurately resolve in a cosmological simulation since the relative force errors can be large and the densities of forming haloes can be very high.

The relaxation probabilities show that at $z = 0$ many particles have completely different energies and orbits compared to their evolution in the mean field limit ($N \rightarrow \infty$). Current cosmological simulations cannot model all the subtle dynamics like orbital resonances which can be important e.g. during tidal stripping (Weinberg 1998). But does relaxation also affect the coarse structure of the object, e.g. their density profiles?

Section (3.3) shows that relaxation heats up and dilutes the central parts of cuspy haloes, and Figure 2 shows that this happens mostly during the early stages of hierarchical structure formation. Is not clear yet how different density profiles of different mass haloes add up when they merge, a series of simulations covering a wide range of parameters would be necessary to clarify this point. Simulations (Barnes 1998, Dekel et al. 2003) and a simple argument based on tidal stripping (Syer & White 1998) suggest that merging similar density profiles reproduces the profile of the progenitors and that a merger with a less cuspy halo has a remnant which is both less cuspy and less concentrated. Thus a final object built up from poorly resolved progenitor haloes could have a shallower cusp slope than it would have in the very large N limit. Qualitatively this agrees also with the result of Binney & Knebe (2002): They used GADGET a tree code similar to PKDGRAV, and MLAPM an adaptive multi-grid code. Two-body relaxation affected their GADGET run stronger and this run showed lower central densities (by about a factor 2) in the two most massive haloes.

At the very least, relaxation provides an explanation for the reason why a given number of particles is needed to resolve the structure of a halo past a certain radius. Relaxation could be the cause of the slow convergence towards an $r^{-1.5}$ cusp in Moore et al. (1999) and Ghigna et al. (2000). Perhaps the mass dependence of relaxation can explain the result of Jing & Suto (2000), who found inner profiles $\propto r^{-1.5}$ for galaxies and $\propto r^{-1.1}$ for clusters, although this result has not been verified by other authors.

ACKNOWLEDGEMENTS

We would like to thank the Swiss supercomputing centre at Manno for computing time where many of these numerical simulations were performed.

REFERENCES

- Barnes J. E., 1998, preprint (astro-ph/9811091)
- Bertin G., 2000, Galactic Dynamics. Cambridge Univ. Press, Cambridge
- Bertschinger E., 2001, ApJSS, 137, 1
- Binney J., Knebe A., 2002, MNRAS, 333, 378
- Binney J., Tremaine S., 1987, Galactic Dynamics. Princeton Univ. Press, Princeton
- Chandrasekhar S., 1942, Principles of Stellar Dynamics. Univ. Chicago Press, Chicago
- Dekel A., Devor J., Hertzroni G., 2003, MNRAS, in press (astro-ph/0204452)
- Fukushige T., Makino J., 2001, ApJ, 557, 533
- Ghigna S., Moore B., Governato F., Lake G., Quinn T., Stadel J., 2000, ApJ, 544, 616
- Hayashi E., Navarro J. F., Taylor J. E., Stadel J., Quinn T., 2003, ApJ, 584, 541
- Hernquist L., 1990, ApJ, 356, 359
- Huang S., Dubinski J., Carlberg R. G., 1993, ApJ, 404, 73
- Jing Y., Suto Y., 2000, ApJ, 529, L69
- Kazantzidis S., Magorrian J., Moore B., 2003, ApJ, in press
- Klypin A., Kravtsov A. V., Bullock J. S., Primack J. R., 2001, ApJ, 554, 903

Navarro J. F., Frenk C. S., White S. D. M., 1996, *ApJ*, 462, 563

Moore B., Governato F., Quinn T., Stadel J., Lake G., 1998, *ApJ*, 499, L5

Moore B., Quinn T., Governato F., Stadel J., Lake G., 1999, *MNRAS*, 310, 1147

Moore B. 2001, In “The dark matter crisis”, AIP Conf. Proc. 586, 73. ed. Martel H. & Wheeler J..

Power C., Navarro J. F., Jenkins A., Frenk C. S., White S. D. M., 2003, *MNRAS*, 338, 14

Spitzer L., 1987, *Dynamical Evolution of Globular Clusters*. Princeton Series in Astrophysics, Princeton

Stadel J., 2001, PhD thesis, U. Washington

Syer D., White S. D. M., 1998, *MNRAS*, 293, 337

Theis C., 1998, *A&A*, 330, 1180

Weinberg M. D., 1998, *MNRAS*, 297, 101

This paper has been typeset from a \TeX / \LaTeX file prepared by the author.